

## **Innovative formulation technology**

### **-Development of a new $\alpha$ -gel emulsification method that provides increased comfort and wrinkle reduction capabilities-**

**Junya Hiyoshi\***; Reiji Miyahara; Yuki Ogura; Taiki Kazama; Yohei Takahashi;

Norinobu Yoshikawa; Kaori Ikuta

MIRAI Technology Institute, Shiseido Co., Ltd., Yokohama, Japan

\*Corresponding author: Junya Hiyoshi, 1-2-11, Takashima, Nishi-Ku, Yokohama 220-0011, Japan, Tel.: +81-45-222-1600, Email: junya.hiyoshi@shiseido.com

### **Abstract**

**Background:** Conventional  $\alpha$ -gels formed by combining surfactants and higher alcohols have been used to stabilize formulations containing moisturizers and emollients. However, to provide sufficient moisturizing power and skin-conditioning effects, these ingredients are highly blended with the conventional  $\alpha$ -gel, which result in stickiness and decreased comfort. One reason is the increased system viscosity owing to the large amount of aqueous phase incorporated between the stacked bilayer structure of the  $\alpha$ -gel. To overcome this problem, a new  $\alpha$ -gel was developed using a two-chain nonionic surfactant, instead of the higher alcohols of conventional  $\alpha$ -gels.

**Methods:** A new  $\alpha$ -gel was constructed using PEG-6 distearate (two-chain nonionic surfactant) and a one-chain hydrophilic surfactant. To confirm its structure, optical and thermal analyses were used.

**Results:** PEG-6 distearate was found to control the width of the lamellar spacing of the laminated structure. Additionally, the new  $\alpha$ -gel contained a greater moisturizer and emollient content than conventional  $\alpha$ -gels because of its unique structure and high stability for polar oils. Applying this  $\alpha$ -gel as an emulsion, skin-softening effects were observed owing to the large amounts of incorporated moisturizers and emollients. Unexpectedly, this emulsion exhibited non-stickiness and a high wrinkle-improving effect after just two weeks of continuous use.

**Conclusion:** A new type of  $\alpha$ -gel was developed by mixing a hydrophilic nonionic surfactant with a two-chain nonionic surfactant. This new  $\alpha$ -gel can contain larger amounts of moisturizers and emollients than conventional  $\alpha$ -gels with high stability and minimal stickiness. Moreover, formulations using this new  $\alpha$ -gel showed strong wrinkle-reduction capability in the short term.

**Keywords:** emulsification;  $\alpha$ -gel; two-chain surfactant; wrinkle reduction

## 1. Introduction

As one of the indicators of skin health, skin softness is closely related to the interaction between keratin fibers and water in the stratum corneum [1]. For this reason, moisturizers have been widely used to retain water in the skin. Certain oils can also have a skin-softening effect, known as the emollient effect [2-3]. These oils are known to act inside the skin, although the mechanism of action has not been comprehensively elucidated. Koike et al. determined that liquid oils soften the skin by interacting with intercellular lipids [4]. Additionally, Nishizaka et al. showed that some polar oils with large solubility parameters interact with keratin in the stratum corneum, which leads to storage of these oils in the skin [5].

Because moisturizers and some oils are capable of softening the skin, various emulsification formulations have been developed to deliver these ingredients to the skin comfortably and effectively. Historically, since the discovery of  $\alpha$ -gels 60 years ago, formulations based on  $\alpha$ -gels consisting of a combination of surfactants and higher alcohols have been widely used in basic cosmetics [6-9]. The surfactants and higher alcohol form a lamellar structure that traps the oil, forming an oil-in-water emulsion, which is the basis of current emulsion and cream formulations. In pursuit of greater moisturizing power and functionality, formulations may contain high quantities of moisturizing ingredients or oils with skin-softening effects, leading to products that are uncomfortable to use daily owing to two factors: the stickiness and instability of the formulation. First, this stickiness is caused by a significant increase in the viscosity of the  $\alpha$ -gel and its applied film. When the aqueous phase in the  $\alpha$ -gel structure contains moisturizers, the lamellar structure in the  $\alpha$ -gel end up containing an excessive amount of the aqueous phase [10,11]. Second, emulsions containing large amounts of highly polar oils with an emollient effect tend to be unstable. This is because the difference in the partitioning of polar oils into the aqueous phase at low and high temperatures leads to non-uniformity of the oil droplet size, known as the Ostwald ripening [12,13].

In this study, the authors developed a new base formulation containing large amounts of emollient oils and moisturizers to overcome these problems. In developing this new base formulation, we were inspired by the role of the two-chain structure of ceramide in enhancing the barrier function of intercellular lipids, specifically by controlling the areal spacing of the stacked structure [14]. A two-chain nonionic surfactant (PEG-6 distearate) was used in place of the higher alcohol of conventional  $\alpha$ -gels to generate a novel  $\alpha$ -gel with a structure that prevents widening of the lamellar spacing. Emulsification formulations based on this novel  $\alpha$ -gel promote the formation of an interface film with a repeating structure of hydrophilic and hydrophobic layers that prevents widening of the lamellar spacing. Therefore, even when moisturizers and polar oils with stratum-corneum softening effects are added at an amount more than twice that of conventional products,

the emulsion exhibits minimal stickiness and high stability. This paper describes the basic properties and skin benefits of this novel  $\alpha$ -gel and its application to emulsification formulations.

## 2. Materials and Methods

### 2.1. Materials

#### 2.1.1. Surfactants and cosmetic raw materials

As the cosmetic-grade two-chain nonionic surfactant, PEG-6 distearate (Emalex 300DI-ST<sup>TM</sup>; Nihon Emulsion Co., Ltd., Saitama, Japan) was used without further purification. As cosmetic-grade hydrophilic surfactants, Ceteth-7 (Emalex-107<sup>TM</sup>; Nihon Emulsion Co., Ltd.), PEG (10) glyceryl stearate (abbreviated as PGS) (Emalex GM-10<sup>TM</sup>, Nihon Emulsion Co., Ltd.), POE (20) hydrogenated castor oil (abbreviated as HCO-20) (Nikkol HCO-20<sup>TM</sup>; Nikko Chemicals Co., Ltd., Tokyo, Japan), POE (10) hydrogenated castor oil (abbreviated as HCO-10) (Emalex HC-10<sup>TM</sup>; Nihon Emulsion Co., Ltd.), and polysorbate-60 (Nikkol TS-10V<sup>TM</sup>; Nikko Chemicals Co.) were used without further purification. Other moisturizers and oils were used as cosmetic ingredients without refining. Ion-exchanged water was used.

#### 2.1.2. Surfactant mixtures

A mixture of PEG-6 distearate and various hydrophilic surfactants were put into a 50-mL screw-cap test tube and then melted at 70 °C. Water was added to the mixture at various ratios, and the mixture was homogenized by repeated stirring and centrifugation at 70 °C. After it was homogenized, the sample was kept at 25 °C for 1 week and used as a measurement sample. Water dispersions of various hydrophilic surfactants alone were also prepared in the same manner.

#### 2.1.3. Sample emulsions

##### i) Cryogenic focused ion-beam scanning electron microscopy (Cryo-FIB-SEM)

Emulsification was performed with reference to D-phase emulsification [15]. First, 0.6 wt% Ceteth-7 and 0.4 wt% PEG-6 distearate were dissolved in 5 wt% dipropylene glycol at 70 °C, and 5 wt% water was added to prepare a D phase. Then, 6 wt% liquid paraffin was emulsified in the D phase at 70 °C to obtain an emulsion. Furthermore, this was added to the remaining aqueous phase components (7 wt% of Dynamite glycerin, 5 wt% of 1,3-Butylene glycol, 0.79 wt% of stabilizing agent and the rest was Ion-exchanged water) to obtain an emulsion.

##### ii) Stability of emulsions against Ostwald ripening

A sample emulsion without the thickener shown in Table 1 and a standard emulsion without PEG-6 distearate were prepared. The above method was used for emulsification. The ratios of HCO-10 and HCO-20 were adjusted, and the hydrophilic–lipophilic balance (abbreviated as HLB) of both emulsions was set to the same level. The total amount of emulsifier in both emulsions was also the same.

**Table 1** Sample emulsions for stability test against Ostwald ripening and their HLB

Ingredients	Concentration (wt%)	
	Sample emulsion	Standard emulsion
HCO-20 (HLB 10.5*)	1.0	0.9
HCO-10 (HLB 7.0*)	0.1	0.6
PEG-6 distearate (HLB 5.0*)	0.4	-
Pentaerythrityl tetraethylhexanoate	10.0	10.0
Dipropylene glycol	5.0	5.0
Ion-exchanged water	78.5	78.5
Total HLB	8.8	9.1

\*HLB values are based on the manufacturer's catalog. The HLB value of the mixture was calculated using the compounding ratio.

### **iii) Texture evaluation by professional panels, atomic force microscopy (AFM) measurements, and home use test (HUT)**

As shown in Table 2, formulations for texture evaluation, AFM measurements, and HUT were prepared. As shown in Table 2(a), two emulsions were prepared using different surfactants and the same amount of oil and moisturizer for texture evaluation by six professional panels. The surfactants in emulsion A were PEG-6 distearate and polysorbate-60 in the weight ratio of 3:7. The surfactants in emulsion B were a traditional  $\alpha$ -gel formulation composed of nonionic surfactants, higher alcohols, and fatty acids.

As shown in Table 2(b), a prototype emulsion containing approximately twice as much emollient and moisturizer as the commercially available product and a commercially available anti-wrinkle emulsion as the control product were used.

**Table 2** Formulations for texture evaluation, AFM measurements, and HUT: (a) Emulsions for texture evaluation by professional panels and (b) the prototype and control emulsions for AFM and HUT.

Ingredients	Concentration (wt%)			
	(a) Emulsions for texture evaluation		(b) Emulsions for AFM and HUT	
	Emulsion A	Emulsion B	Prototype emulsion	Control emulsion
Ion-exchanged water	48.91	46.50	50.0	64.31
95% EtOH	5.0	5.0	5.0	5.0
Surfactants	1.0	1.0	1.0	1.2
Wax	6.0	6.0	2.0	1.0
Oils of softening stratum corneum	-	-	5.0	2.0
Polar oils	8.0	8.0	5.0	6.5
Non-polar oils	5.0	5.0	3.3	2.0
Silicon oils	3.0	3.0	4.5	6.0
Higher alcohols	-	0.24	-	0.9
Fatty acids	-	2.3	-	-
Humectants	22.0	22.0	21.5	10.1
Thickeners	0.22	0.22	0.56	0.24
Other ingredients	0.87	0.87	2.14	0.75

## 2.2. Methods

### 2.2.1. Differential scanning calorimetry (DSC)

Approximately 5 mg of sample was placed in an aluminum pan and heated from 30 to 80 °C at a rate of 2 °C/min in a differential scanning calorimeter (DSC1, Mettler Toledo, Greifensee, Switzerland).

### 2.2.2. Small- and wide-angle X-ray scattering (SWAXS) measurement

The concentrations of the surfactant dispersion systems described above were changed from 25 to 50 wt%, and the lamellar space of the gel and liquid-crystal phases were investigated using SWAXS. Samples were filled in a capillary cell for SWAXS (SAXSess mc<sup>2</sup>, Anton Paar, Graz, Austria) measurements.

According to the Bragg equation (1), there is the relationship between the interlayer spacing  $d$  of the gel phase and the position  $q^*$  of the magnitude of the scattering vector corresponding to the position where a sharp reflection peak is observed.

$$\hat{q}^* = 2\pi/d \quad (1)$$

The lamellar spacing was calculated using this formula.

### 2.2.3. Cryo-FIB-SEM

Samples were filled in a sample holder, plunged with the preparation, and rapidly frozen in slush nitrogen for Cryo-FIB-SEM (Thermo Fisher Scientific, Inc.,

Massachusetts, USA) observations.

(1) Protective film deposition conditions

Pre-chamber deposition film: Pt sputter coater 10–20 mA, 100–200 s

(2) FIB processing conditions

Sample tilt angle: 52°

(3) SEM observation conditions

Acceleration voltage: 1–5 kV

Sample tilt angle 0° and 52°

Detector: TLD, BSE mode

Observation temperature and stage temperature: -120 °C or less

#### **2.2.4. Stability testing of emulsions**

The test and control formulations shown in Table 1 were maintained at a constant temperature of 50 °C and also subjected to temperature cycling in which the temperature was raised and lowered at 10 °C/h in the range of 5 °C to 45 °C and held at 5 °C and 45 °C for 2 h. After one month of heat treatment, microscopic observation was performed.

#### **2.2.5. AFM measurements for Young's modulus of human stratum corneum**

The Young's modulus of the stratum corneum was determined using AFM. Tape-stripped stratum corneum was used for the skin and coated with the prototype emulsion or control emulsion. The area per sample was 2.5 cm × 2.5 cm, and the application volume was 2 µL/cm<sup>2</sup> on the basis of the standard application volume of emulsion products. The area to be sampled was washed with soap and allowed to acclimate for 15 min at 23 °C and 50% humidity. After acclimatization, the sample was applied to this area and allowed to acclimate for 5 min. Then, by performing 10 round-trip tissue-offs at a constant force, the first layer of the stratum corneum was tape stripped. The Young's modulus of the human stratum corneum was measured using a probe microscope (Dimension Icon XR, Bruker) with a probe tip (RTE SPA300-30, Bruker) of 30 nm in radius in the force volume mode. The measurement range was 50 µm × 50 µm with 32 × 32 dots, and the force curve at each point was acquired. The Young's modulus was calculated by fitting the obtained force curve indentation using the Derjaguin–Muller–Toporov (DMT) theory [16].

### **2.3. Texture evaluation of new and conventional α-gel formulas**

Texture evaluation was conducted by six professional panels. Emulsion B in Table 2(a) was placed in the center “0”. Seven grades from -3 to +3 were used for Emulsion A.

## 2.4. Human panel test and home use test (HUT)

The panel consisted of a total of 120 people in their 40s and 60s, with N=60 per sample. The duration of the home use test was 2 weeks. Questionnaires were taken to evaluate usability and changes in daily skin. A total number of 36 people were randomly selected from the HUT panel to avoid any variation in age, and the panel test was conducted before use and after one week of continuous use. The skin surface conditions were captured by a video microscope [17] after washing the face with soap at a constant temperature and humidity and after 15 min of acclimatization. The fineness of the skin surface as revealed by the number of ridges was calculated by image analysis. The HUT questionnaire was rated on a 5-point scale. These protocols for human studies were approved by Shiseido Research Ethics Committee of Shiseido Global Innovation Center (Yokohama, Japan).

## 3. Results

### 3.1. Characterization of new $\alpha$ -gel system and development of new $\alpha$ -gel formulation

#### 3.1.1. Self-assemblies of 50 wt% aqueous dispersions of various surfactant mixtures

Various hydrophilic surfactants and PEG-6 distearate were mixed at a mixing ratio of 6:4 to make a 50 wt% water dispersion. The DSC thermogram of each sample is shown in Figure 1. As shown in Figure 1, the aqueous dispersion of each surfactant mixture became self-assemblies with one co-melting point. The co-melting point was confirmed as the gel–liquid crystal transition temperature using SWAXS measurements at different temperatures.

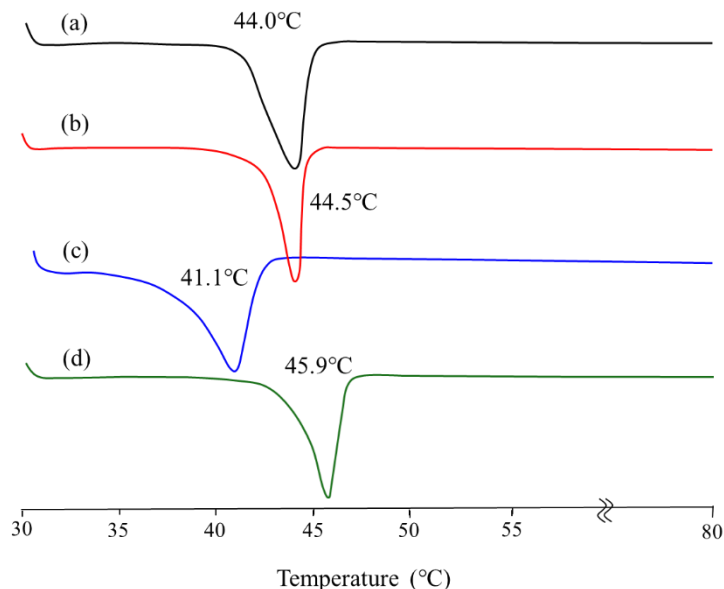


**Figure 1** DSC thermograms of various PEG-6 distearate mixtures: (a) 50 wt% aqueous dispersion of Ceteth-7:PEG-6 distearate (6:4), (b) 50 wt% aqueous dispersion of

PGS:PEG-6 distearate (6:4), (c) 50 wt% aqueous dispersion of HCO-20:PEG-6 distearate (6:4), and (d) 50 wt% aqueous dispersion of polysorbate 60:PEG-6 distearate (6:4). Each mixture has only one eutectic point.

The SWAXS diffraction pattern of each self-assembled material at 20 °C is shown in Figure 2. In this figure, the regular peaks ( $\blacktriangledown$ ) on the small-angle side in the ratio of 1:2:3 represent the lamellar structure. The peak ( $\blacktriangledown$ ) near the scattering vector ( $q$ ) of 15 nm<sup>-1</sup> indicates that the sublattice plane is hexagonal. In other words, all the self-assembled materials exhibited the  $\alpha$ -gel structure [17]. In conjunction with Figure 1, all water dispersions of mixtures (6:4) of various hydrophilic surfactants and PEG-6 distearate formed  $\alpha$ -gels with a co-melting point. Interestingly, the 50 wt% aqueous dispersion of HCO-20 alone resulted in a lamellar liquid crystal with no gel–liquid crystal transition temperature, although the addition of PEG-6 distearate transformed it into an  $\alpha$ -gel. In the other self-assemblies, the peak near 15 nm<sup>-1</sup> ( $\blacktriangledown$ ) was greatly sharpened.

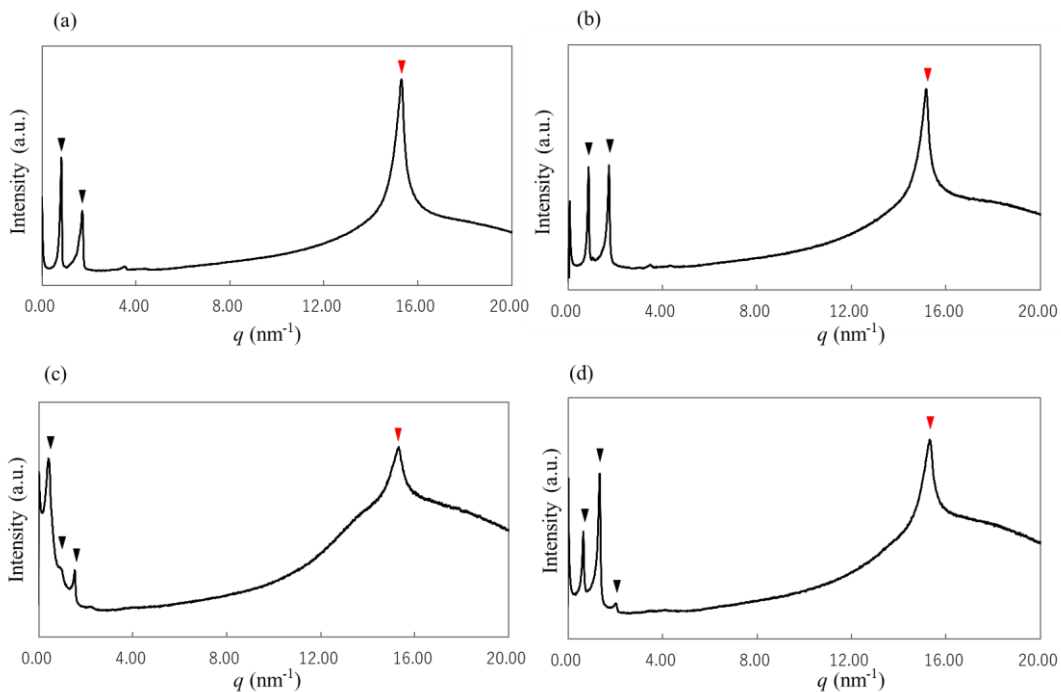


**Figure 2** SWAXS diffraction patterns of various gels at 20 °C: (a) 50 wt% aqueous dispersion of Ceteth-7:PEG-6 distearate (6:4), (b) 50 wt% aqueous dispersion of PGS:PEG-6 distearate (6:4), (c) 50 wt% aqueous dispersion of HCO-20:PEG-6 distearate (6:4), and (d) 50 wt% aqueous dispersion of polysorbate 60:PEG-6 distearate (6:4). The peaks ( $\blacktriangledown$ ) that appear regularly in the ratio of 1:2:3:4 on the small-angle side represent the lamellar structure. The peak near 15 nm<sup>-1</sup> ( $\blacktriangledown$ ) indicates that the sublattice plane is hexagonal. Each aqueous dispersion of a mixture of hydrophilic detergent and PEG-6 distearate (6:4) formed an  $\alpha$ -gel.

### 3.1.2. Gel–liquid crystal transition temperature and enthalpy change by mixing PEG-6 distearate

Table 3 shows the gel–liquid crystal transition temperatures and enthalpies of melting for 50 wt% water dispersions of various hydrophilic surfactants alone in addition with those for mixtures of PEG-6 distearate. The melting point and enthalpy of 100 wt% PEG-6 distearate are also listed in Table 3. As shown in Table 3, the gel–liquid crystal transition temperature increased by approximately 5 °C for each mixture. For HCO-20, which only formed lamellar liquid crystals, the gel–liquid crystal transition temperature arising from the  $\alpha$ -gel was observed. Additionally, the melting enthalpies increased in all mixtures.

**Table 3** Gel–liquid crystal transition temperature and enthalpy of each surfactant mixture

Samples	Gel–liquid crystal transition temperature (°C)	Enthalpy (J/g)
50 wt% Ceteth-7	39.45 ± 0.03*	8.42 ± 0.42
50 wt% Ceteth-7:PEG-6 distearate (6:4)	44.02 ± 0.09	28.36 ± 0.38
50 wt% PGS	40.26 ± 0.09	13.37 ± 1.31
50 wt% PGS:PEG-6 distearate (6:4)	44.52 ± 0.20	26.52 ± 0.64
50 wt% HCO-20	N.D.**	N.D.
50 wt% HCO-20:PEG-6 distearate (6:4)	41.09 ± 0.09	12.79 ± 0.18
50 wt% Polysorbate 60	40.53 ± 0.09	1.01 ± 0.38
50 wt% Polysorbate 60:PEG-6 distearate (6:4)	45.89 ± 0.07	22.19 ± 1.15
100 wt% PEG-6 distearate***	38.70 ± 0.11	80.74 ± 6.26

\*The mean value measured three times and  $\pm$  represent the standard deviation.

\*\*N.D. means Not Detected.

\*\*\*Since PEG-6 distearate does not disperse in water, the melting point at 100 wt% is described.

### 3.1.3. Changes in lamellar spacing from changes in the concentration of the surfactant mixtures

The lamellar surface spacing was measured at decreasing concentrations for the mixture of Ceteth-7 and PEG-6 distearate and the mixture of PGS and PEG-6 distearate, which showed sharp SWAXS peaks representing the lamellar structure. There was no significant increase in the lamellar spacing with water dilution in both systems compared with the previously reported lamellar spacing of  $\alpha$ -gels constructed with higher alcohols and surfactants [10, 11]. Specifically, at 50% concentration of the mixture in the aqueous phase, both mixtures had lamellar spacings of almost 7.5 nm. Additionally, at 25% concentration of the mixture in the aqueous phase, the mixture of Ceteth-7 and PEG-6 distearate had a lamellar spacing of 10 nm, and the mixture of PGS and PEG-6 distearate had a lamellar spacing of 8.5 nm. An increase of approximately only 1-2 nm in the areal spacing owing to water incorporation was observed in both mixtures. However, at the same concentration, the previously reported lamellar spacing of  $\alpha$ -gels [10, 11] is

approximately 20 nm.

### 3.1.4. Morphological observation of emulsified droplets

Cryo-FIB-SEM images of the sample emulsion are shown in Figure 3. Figure 3(a) shows a magnified view of a non-spherical droplet, and Figure 3(b) shows a magnified view of a shelly-edged droplet. As shown in Figure 3(a), snaggle-shaped oil droplets were observed in this emulsion. Furthermore, Figure 3(b) shows non-spherical oil droplets and a raised shell at the oil–water interface.

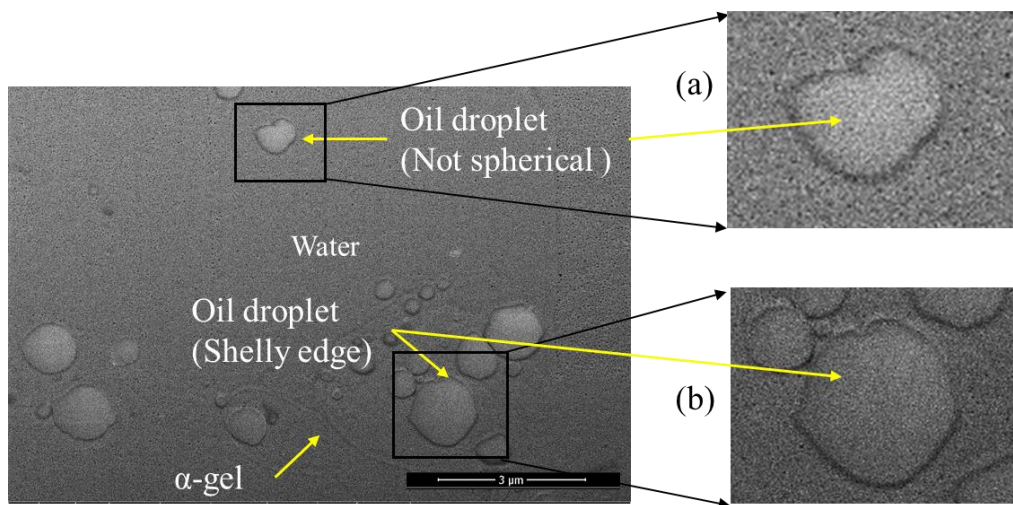


**Figure 3** Cryo-FIB-SEM images of the sample emulsion: (a) Enlarged view of a non-spherical oil droplet and (b) enlarged view of a shelly-edged oil droplet.

### 3.1.5. Stability against Ostwald ripening for emulsification

Figure 4 shows 400 $\times$  micrographs of the emulsified state of the emulsions prepared using the formulas given in Table 1 at day 1, after 1 month at 50 °C, and after 1 month of temperature cycling at 5–45 °C/day. Figure 4(a) shows images of the sample emulsion and Figure 4(b) shows images of the control emulsion. As shown in Figure 4(a), the sample emulsion containing PEG-6 distearate did not easily expand, even after it was subjected to the temperature cycle and maintained at 50 °C, conditions under which Ostwald ripening was likely to occur. However, as shown in Figure 4(b), the standard emulsion without PEG-6 distearate showed enlarged oil droplets after it was subjected to the temperature cycle and maintained at 50 °C.

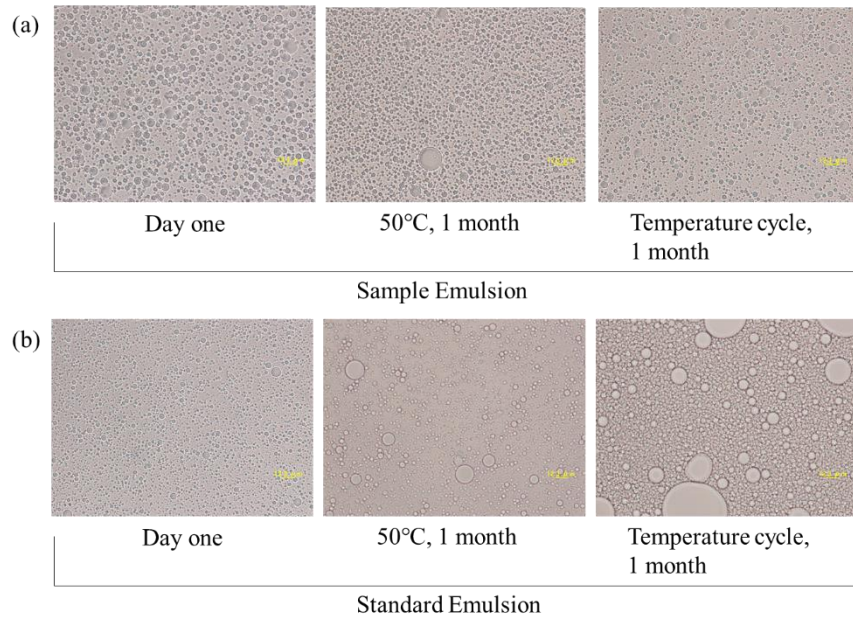


**Figure 4** Micrographs ( $\times 400$ ) of emulsions (formulas given in Table 1) at day 1, after 1 month at  $50^{\circ}\text{C}$ , and after 1 month of temperature cycling: (a) Sample emulsion and (b) standard emulsion.

### 3.1.6. Texture evaluation by professional panels

Because  $\alpha$ -gels formed using one-chain hydrophilic surfactants and two-chain surfactants are insoluble in polar oils and water, they attach to the oil–water interface to form the emulsions shown in Table 2(a). Emulsion A was prepared using the new  $\alpha$ -gel, and emulsion B was prepared using a conventional  $\alpha$ -gel. Interestingly, emulsion A was found to be less sticky (the average score was -1.5 relative to that of emulsion B) and to blend into the skin faster than emulsion B (the average score was +1.8), even though both emulsions A and B contained the same amounts of moisturizers and emollients.

## 3.2. Development of an innovative formula and its effect on the skin surface

### 3.2.1. Development of an innovative formula with stratum-corneum softening effect

Ozawa et al. reported that emollients with high polarity exhibit high stratum-corneum softening effects [3]. As shown in Table 2(b), the commercially available anti-wrinkle emulsion was used as the control, and the prototype emulsion containing twice the amounts of emollients and moisturizers was prepared using the novel  $\alpha$ -gel developed in this study. The stratum-corneum softening effect of the prototype emulsion and control emulsion was examined using AFM measurements of the human stratum corneum. Figure 5 shows a comparison of the Young's modulus of tape-stripped stratum corneum, where warm colors indicate softening [19]. As shown in Figure 5, the prototype emulsion softened the stratum corneum more than the control emulsion.

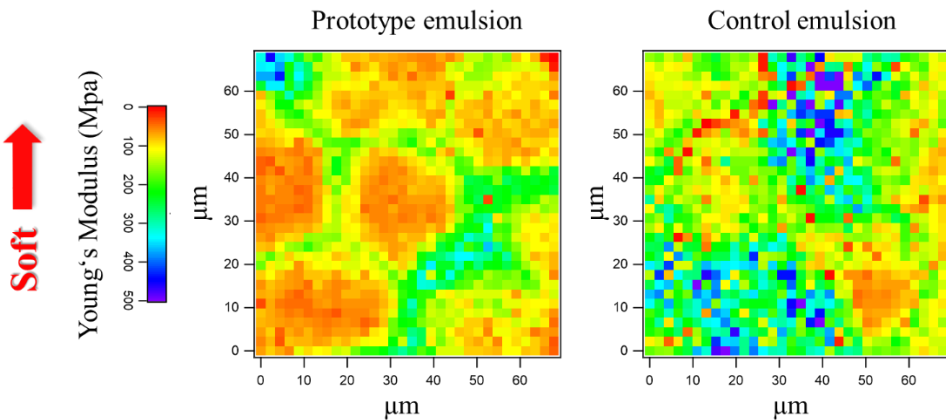


**Figure 5** Measurement results of human stratum corneum softness using AFM indentation depth as an index. Warmer colors correspond to softening (low Young's modulus), while colder colors indicate hardening (high Young's modulus).

### 3.2.2. Evaluation of penetration feeling after continuous use

The average penetration scores, obtained through questionnaires, for the prototype emulsion and control emulsion shown in Table 2(b) after single use were 3.5 and 3.6, respectively. However, interestingly, although the prototype emulsion contained more than twice the amounts of moisturizer and emollient as the control emulsion, it showed the same degree of penetration feeling as the control emulsion after single use.

### 3.2.3. Improvement of skin surface condition before and after continuous use

Figure 6 shows the improvement rate of the skin surface condition by using the prototype and control emulsion (formulas given in Table 2(b)) before and after continuous use for 1 week, obtained through video microscope observations, specifically the improvement rates of the number of skin surface furrows (Figure 6(a)) and the roughness of the skin surface (Figure 6(b)). As shown in Figure 6(a), both emulsions resulted in a significant increase in the number of skin surface furrows after continuous use. However, the roughness of the skin surface was significantly improved only after using the prototype emulsion, as shown in Figure 6(b).

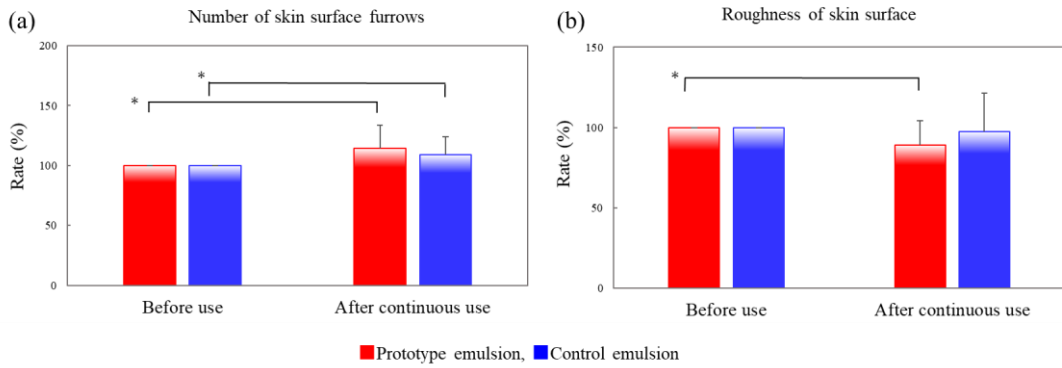


**Figure 6** Improvement of skin surface: (a) Number of skin surface furrows and (b) roughness of the skin surface. The red bar represents the prototype emulsion. The blue bar represents the control emulsion. The unpaired student's t-test was conducted to compare the data for before use and after continuous use. The number of panels in each group was 18. Statistical significance ( $p < 0.05$ ) is marked by \*. Values are presented as mean  $\pm$  standard deviation.

### 3.2.4. Improvement of wrinkles

The prototype emulsion was perceived to have a higher skin softening and wrinkle improvement effect than the control emulsion. In the questionnaire, the total number of panels whose scores for the wrinkle-improvement-related questions increased by 5 points or more after continuous use was 3 out of 17 for the control emulsion and 9 out of 18 for the prototype emulsion. As shown in Figure 7, for a prime example, the total wrinkle improvement score was +9. As shown in Figure 7, the wrinkles were indeed reduced after continuous use. Additionally, the enlarged image showed that many fine wrinkles (indicated by green arrows) appeared, rendering the large wrinkles (indicated by orange arrows) less noticeable.

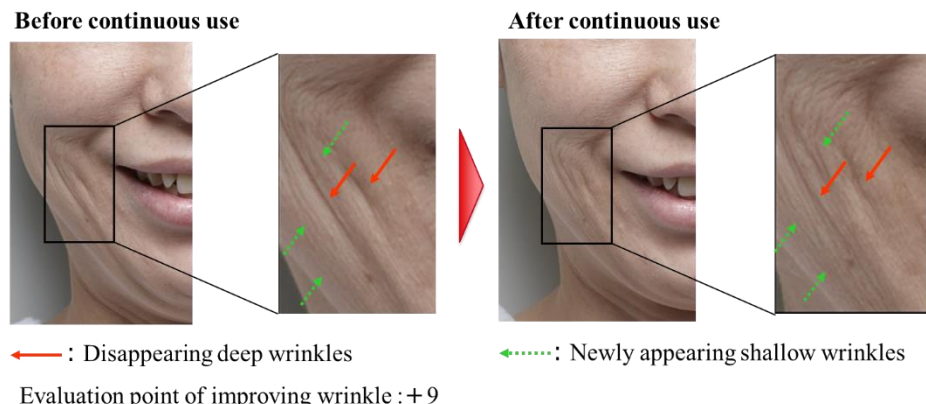


**Figure 7** Photographs of a 40-year-old Japanese woman before and after continuous use of the prototype emulsion to compare the expression wrinkles on her cheeks. The right

photograph is an enlarged view. The total wrinkle improvement score based on an individual evaluation was +9.

In terms of the relationship between the degree of improvement of fine wrinkles at the corners of the eyes and the degree of improvement of skin softness, there was some correlation after using the prototype emulsion. The correlation coefficient for the prototype emulsion was 0.46, indicating some correlation. However, the correlation coefficient for the control emulsion was 0.17, indicating few correlations.

## 4. Discussion

### 4.1. Investigation and applying the new $\alpha$ -gel for emulsification

#### 4.1.1. Confirmation of the formation of an $\alpha$ -gel structure

The following phenomena were observed in the self-assemblies formed using various hydrophilic surfactants with single-chain alkyl groups and PEG-6 distearate. First, from the results of DSC measurements shown in Table 3, the melting enthalpy and gel–liquid crystal transition temperature of self-assemblies increased in the presence of PEG-6 distearate. In addition, the SWAXS results (Figure 2) showed that the hexagonal structure of the  $\alpha$ -gel became rigid in the presence of PEG-6 distearate. From these results, these self-assemblies were confirmed to form  $\alpha$ -gel structures with a more rigid structure than that of conventional ones. On the other hand, ceramide, which has two-chain alkyl groups, similar to PEG-6 distearate, exists in intercellular lipids with these alkyl groups spread between planes to form an anchor-link-like structure [14]. Considering its unique structure, PEG-6 distearate is capable of adopting an anchoring structure, with the hydrophobic groups of the two-chain alkyl groups spread between hydrophobic surfaces to strengthen these self-assemblies.

#### 4.1.2. Applying this new $\alpha$ -gel structure for new base formulas

The emulsified particles formed by this self-assembly were in the form of oil droplets (shown in Figure 3). Considering that the spacing of these lamellar surfaces did not widen, these oil droplets were likely covered by a thin film of the  $\alpha$ -gel. In contrast, conventional  $\alpha$ -gel systems [10,11] show a large increase in the areal spacing with water dilution. Because this emulsion particle did not enlarge after heat treatments (shown in Figure 4), specifically temperature cycling and high temperature, the thin film of this  $\alpha$ -gel likely had a repeating structure of hydrophilic and hydrophobic layers, which was impermeable to the encapsulated oil. Thus, this high stability against Ostwald ripening suggests that the repeating structure of this strong interfacial film is impermeable to oil, even polar oils.

#### 4.1.3. Possibility of an innovative formula with high concentrations of moisturizers

## **and emollients**

The emulsion (formular given in Table 2(a)) constructed from this new  $\alpha$ -gel was less sticky and penetrated the skin faster than a conventional  $\alpha$ -gel emulsion, even though both emulsions contained the same amounts of moisturizer and emollient. These characteristics of the new formulation are derived from the unique feature of the new  $\alpha$ -gel. In other words, unlike conventional  $\alpha$ -gel systems, the viscosity of the developed system does not increase because water and moisturizers cannot enter the lamellar spacing even if it contains a large amount of moisturizer. Therefore, the viscosity does not increase even during the application process, and the product exhibits a non-sticky feeling. As shown in Figure 4, the oil did not permeate through the film because the oil droplets were surrounded by a strong interfacial film. Additionally, emollients, the source of stickiness, did not appear on the film surface during the application process.

### **4.2. Functionality of the new $\alpha$ -gel formulation and skin improving effect**

#### **4.2.1. Development of a new $\alpha$ -gel formulation with stratum-corneum softening effect**

As shown in Figure 5, the prototype emulsion (formular given in Table 2(b)) showed a higher stratum-corneum softening effect than the control emulsion. This result suggests that the moisturizers and emollients, present in large amounts in the formulation, interacted well with the stratum corneum. However, this prototype emulsion showed the same penetration feeling as the control emulsion, even though it contained more than twice the amounts of moisturizer and emollient as the control emulsion. Considering that the penetration feeling conflicted with the feeling of remaining on the skin and stickiness, the prototype emulsion should exhibit the same level of after-skin feeling as the control emulsion. Therefore, the emulsification product using this new  $\alpha$ -gel system leads to a significant reduction in stickiness and the feeling of remaining on the skin, derived from moisturizers and emollients, after application. Given that the emollients, the basis of the stratum-corneum softening effect, were highly polar oils, this new emulsification product had strengths in usability and in stability against polar oils, characteristics absent from conventional  $\alpha$ -gel emulsification products. This new  $\alpha$ -gel emulsification product contains more than twice the amounts of moisturizers and emollients as conventional  $\alpha$ -gel emulsification products without sacrificing usability, thus enabling the development of innovative emulsification formulations that demonstrate high stratum-corneum softening effects.

#### **4.2.2. Improvement of skin surface and wrinkles**

There are reports of findings related to skin surface shape, softness, and wrinkle formation. Shiihara et al. reported that numerous skin surface furrows prevent the

formation of wrinkles [20], while Hara et al. reported that the softness of skin surface prevents the formation of wrinkles [21]. Additionally, according to the report by Ogura et al. in IFSCC 2020, wrinkles are formed by age-related hardening of the stratum corneum and loosening of the dermis layer [22]. Therefore, as shown in Figure 6, it was inferred that softening of the stratum corneum by moisturizers and emollients increases the number of skin surface furrows, which eliminates the distortion of the large stratum corneum leading to wrinkles, thus reducing the number of deep wrinkles shown as Figure 7. Additionally, there was a correlation between the degree of improvement in skin softness and the degree of improvement in fine wrinkles at the corners of the eyes, indicating that those who felt their skin had become softer felt their fine wrinkles had improved. These results suggest that skin surface shaping and softening has a positive impact on both wrinkle elimination and the perception of the issue of wrinkles, which is often difficult to assess.

## 5. Conclusion

In this study, we developed a new  $\alpha$ -gel with controlled interfacial film spacing by mixing a hydrophilic nonionic surfactant and a two-chain nonionic surfactant. This  $\alpha$ -gel differs significantly from conventional  $\alpha$ -gels in that it forms strong interfacial films without widening of the lamellar spacing. This enables the stable incorporation of large amounts of moisturizers and emollients without compromising the texture. Emulsions based on this new  $\alpha$ -gel can contain more than twice the amounts of moisturizers and emollients than emulsions based on conventional  $\alpha$ -gels to provide a high stratum-corneum softening effect. This effect leads to improved skin softness and skin surface furrows, thus enhancing wrinkle elimination. Therefore, this new  $\alpha$ -gel has the potential to maximize the emotional and functional value of moisturizers and emollients by allowing the incorporation of higher concentrations of these ingredients in emulsification formulations, which has not been possible with conventional  $\alpha$ -gels. Thus, this new  $\alpha$ -gel is expected to facilitate the creation of innovative cosmetics that can deliver enhanced skin benefits while providing a comfortable usage experience to consumers.

## Conflict of Interest Statement

NONE

## References

1. Jokura Y, Ishikawa S, Tokuda H, Imokawa G (1995) Molecular analysis of elastic properties of the stratum corneum by solid-state  $^{13}\text{C}$ -nuclear magnetic resonance spectroscopy. *J Invest Dermatol* 104:806-812.
2. Miyahara R (2017) Emollients. *Cosmetic Science and Technology: Theoretical Principles and Applications*, Sakamoto K, Lochhead R, Maibach H, Yamashita Y (Eds), Elsevier Science Publishing Co., New York, pp. 245-253.
3. Ozawa T, Nishiyama S, Kumano Y (1987) Water and Cosmetics. *J Soc Cosmet Chem Jpn* 11(4):297-307.
4. Koike T, Nakajima N, Okumura Hideharu, Okumura, Hidenobu (2011) Skin Softening Mechanism of Liquid oil. *J Soc Cosmet Chem Jpn* 45(1):14-21.
5. Nishizaka T, Yamazaki S (1998) Screening of skin penetration oil for cosmetics. *Drug Delivery System* 13(5):347-351.
6. Fukushima S, Yamaguchi M, Harusawa F (1975) Effect of long chain alcohols on stabilization of oil-in-water emulsion. *J Colloid Interface Sci* 51(3):548-549.
7. Junginger HE (1984) Colloidal structures of O/W creams. *Pharmaceutisch Weekblad* 6:141-149.
8. Uyama M, Ikuta K, Teshigawara T, Watanabe K, Miyahara R (2013) The viscosity stability of O/W emulsion containing  $\alpha$ -gel through an ionic-complex system. *J Oleo Sci* 62:9-16.
9. Akatsuka H, Ohara Y, Otsubo Y (2006) Effects of dimethyl ammonium chloride on the rheological behavior of behenyl trimethyl ammonium chloride/1-hexadecanol/water ternary system. *J Colloid Interface Sci* 302:341-346.
10. Watanabe K, Inoue H, Teshigawara T, Kimura T (2012)  $\alpha$ -Gel Prepared in Sodium Methyl Stearoyl Taurate / Behenyl Alcohol / Water System-Characterization of Structural Changes with Water Concentration. *J. Oleo Sci* 61:29-34.
11. Orita M, Uchiyama M, Hanamoto T, Yamashita O, Naitou S, Takeuchi K, Katayama Y, Tanabe H, Fukuda K, Okada J (2012) Formation of Pseudo-Intercellular Lipids Membrane on the Skin Surface by the Alpha-Gel Holding a Large Amount of Water. *J Soc Cosmet Chem Jpn* 46(1):25-32.
12. Yamashita Y, Miyahara R, Sakamoto K (2017) Emulsion and Emulsification Technology. *Cosmetic Science and Technology: Theoretical Principles and Applications*, Sakamoto, K, Lochhead, R, Maibach H, Yamashita Y (Eds), Elsevier Science Publishing Co., New York, pp. 489-506.
13. Taylor P (1995) Ostwald ripening in emulsions. *Colloids and Surfaces A*, 99:175-185.
14. Iwai I, Han H, Hollander L, Svensson S, Ödenfelt L, Anwar J, Brewer J, Bloksgaard M, Laloeuf A, Nosek D, Masich S, Bagatolli L, Skoglund U, Norlén L (2012) The

Human Skin Barrier Is Organized as Stacked Bilayers of Fully Extended Ceramides with Cholesterol Molecules Associated with the Ceramide Sphingoid Moiety. *J Invest Dermatology* 132:2215–2225.

15. Sagitani H, (1992) Phase-Inversion and D-Phase Emulsification. *Organized Solutions*, Friberg, SE, Lindman B(Eds), Marcel Dekker, New York, pp 259–271.
16. Derjaguin BV, Muller VM, Toporov Yu P (1975) Effect of contact deformations on the adhesion of particles. *J Colloid Interface Sci* 53:314-326.
17. Masuda U, Hirao T, Mizunuma H (2013), Improvement of skin surface texture by topical estradiol treatment in climacteric women. *J Derma Treat* 24: 312-317.
18. Iwata T (2017), Lamellar Gel Network. *Cosmetic Science and Technology: Theoretical Principles and Applications*, Sakamoto, K, Lochhead, R, Maibach, H, Yamashita, Y(Eds), Elsevier Science Publishing Co., New York, pp.415-447.
19. Yuan Y, Verma R (2006), Measuring microelastic properties of stratum corneum. *Colloids and Surfaces B: Biointerfaces* 48:6-12.
20. Shiihara, Y, Sato, M, Hara Y, Iwai, I, Yoshikawa N (2015) Microrelief suppresses large wrinkling appearance: an in silico study. *Skin Research and Technology* 21:4-191.
21. Hara, Y, Sato, M, Shiihara, Y, Yoshikawa, N, Hirao, T, Iwai I (2017) Involvement of Stratum Corneum in Initial Residual Wrinkle Formation Induced by Facial Expression. *28th IFSCC Magazine* 1:15-22.
22. Ogura, Y, Hara, T, Ninomiya, M, Yamashita, T, Katagiri, C, Kobayashi, K, Shiihara, Y, Hozumi N (2020) Emergence of Eye Wrinkles Can Be Controlled By Balancing The Elasticity of The Stratum Corneum and The Dermis. *31th IFSCC Congress* in press